Carbon Dioxide Capture for Storage in Deep Geologic Formations – Results from the CO_2 Capture Project

Capture and Separation of Carbon Dioxide from Combustion Sources

Edited by

David C. Thomas
Senior Technical Advisor
Advanced Resources International, Inc.
4603 Clearwater Lane
Naperville, IL, USA

Volume 1

ELSEVIER
2005

Amsterdam – Boston – Heidelberg – London – New York – Oxford
Paris – San Diego – San Francisco – Singapore – Sydney – Tokyo

Elsevier Internet Homepage – http://www.elsevier.com
Consult the Elsevier homepage for full catalogue information on all books, major reference works, journals, electronic products and services.

Elsevier Titles of Related Interest

AN END TO GLOBAL WARMING
L.O. Williams
ISBN: 0-08-044045-2, 2002

FUNDAMENTALS AND TECHNOLOGY OF COMBUSTION
F. El-Mahallawy, S. El-Din Habik
ISBN: 0-08-044106-8, 2002

GREENHOUSE GAS CONTROL TECHNOLOGIES: 6TH INTERNATIONAL CONFERENCE
John Gale, Yoichi Kaya
ISBN: 0-08-044276-5, 2003

MITIGATING CLIMATE CHANGE: FLEXIBILITY MECHANISMS
T. Jackson
ISBN: 0-08-044092-4, 2001

Related Journals:
Elsevier publishes a wide-ranging portfolio of high quality research journals, encompassing the energy policy, environmental, and renewable energy fields. A sample journal issue is available online by visiting the Elsevier web site (details at the top of this page). Leading titles include:

Energy Policy
Renewable Energy
Energy Conversion and Management
Biomass & Bioenergy
Environmental Science & Policy
Global and Planetary Change
Atmospheric Environment
Chemosphere – Global Change Science
Fuel, Combustion & Flame
Fuel Processing Technology

All journals are available online via ScienceDirect: www.sciencedirect.com

To Contact the Publisher
Elsevier welcomes enquiries concerning publishing proposals: books, journal special issues, conference proceedings, etc. All formats and media can be considered. Should you have a publishing proposal you wish to discuss, please contact, without obligation, the publisher responsible for Elsevier's Energy program:

Henri van Dorssen
Publisher
Elsevier Ltd
The Boulevard, Langford Lane
Kidlington, Oxford
OX5 1GB, UK

Phone: +44 1865 84 3682
Fax: +44 1865 84 3931
E.mail: h.dorssen@elsevier.com

General enquiries, including placing orders, should be directed to Elsevier's Regional Sales Offices – please access the Elsevier homepage for full contact details (homepage details at the top of this page).

ELSEVIER B.V.
Radarweg 29
P.O. Box 211, 1000 AE Amsterdam
The Netherlands

ELSEVIER Inc.
525 B Street, Suite 1900
San Diego, CA 92101-4495
USA

ELSEVIER Ltd
The Boulevard, Langford Lane
Kidlington, Oxford OX5 1GB
UK

ELSEVIER Ltd
84 Theobalds Road
London WC1X 8RR
UK

First edition 2005

Library of Congress Cataloging in Publication Data
A catalog record is available from the Library of Congress.

British Library Cataloguing in Publication Data
A catalogue record is available from the British Library.

ISBN: 0-08-044570-5 (2 volume set)

Volume 1: Chapters 8, 9, 13, 14, 16, 17, 18, 24 and 32 were written with support of the U.S. Department of Energy under Contract No. DE-FC26-01NT41145. The Government reserves for itself and others acting on its behalf a royalty-free, non-exclusive, irrevocable, worldwide license for Governmental purposes to publish, distribute, translate, duplicate, exhibit and perform these copyrighted papers. EU co-funded work appears in chapters 19, 20, 21, 22, 23, 33, 34, 35, 36 and 37. Norwegian Research Council (Klimatek) co-funded work appears in chapters 1, 5, 7, 10, 12, 15 and 32.

Volume 2: The Storage Preface, Storage Integrity Preface, Monitoring and Verification Preface, Risk Assessment Preface and Chapters 1, 4, 6, 8, 13, 17, 18, 19, 20, 21, 22, 23, 24, 25, 26, 27, 28, 29, 30, 31, 32, 33 were written with support of the U.S. Department of Energy under Contract No. DE-FC26-01NT41145. The Government reserves for itself and others acting on its behalf a royalty-free, non-exclusive, irrevocable, worldwide license for Governmental purposes to publish, distribute, translate, duplicate, exhibit and perform these copyrighted papers. Norwegian Research Council (Klimatek) co-funded work appears in chapters 9, 15 and 16.

♾ The paper used in this publication meets the requirements of ANSI/NISO Z39.48-1992 (Permanence of Paper).
Printed in The Netherlands.

Carbon Dioxide Capture for Storage in Deep Geologic Formations, Volume 1
D.C. Thomas and S.M. Benson (Eds.)

Chapter 34

DEVELOPMENT OF OXYGEN CARRIERS FOR CHEMICAL-LOOPING COMBUSTION

Juan Adánez, Francisco García-Labiano, Luis F. de Diego, Pilar Gayán, Alberto Abad and Javier Celaya

Instituto de Carboquímica (CSIC), Department of Energy and Environment, Miguel Luesma Castán 4, 50015 Zaragoza, Spain

ABSTRACT

The objective of this work was to develop oxygen carriers with enough reduction and oxidation rates, resistant to the attrition and with high durability, maintaining the chemical, structural and mechanical properties in a high number of reduction–oxidation cycles, to be used in a chemical-looping combustion (CLC) system. A significant number of oxygen carriers, composed up to 80% of Cu, Fe, Mn or Ni oxides on Al_2O_3, sepiolite, SiO_2, TiO_2 or ZrO_2, were prepared by different methods, and tested in a thermogravimetric analyser (TGA) and in a fluidized bed. Based on data of crushing strength, reactivity, attrition, and agglomeration of the carriers and its variation during successive reduction–oxidation cycles, the three most promising oxygen carriers based on Cu, Fe, and Ni were selected and prepared to be tested in a pilot plant.

The effect of the main operating variables, such as temperature, gas composition, gas concentration, etc. on the reduction and oxidation reaction rates were analysed in a TGA to determine the kinetic parameters of the selected carriers. A heat balance in the particle showed that the particles can be considered isothermal when using small particle sizes, as it would be normal in a CLC process. The reduction reaction rate of the oxygen carriers with CH_4 was controlled by the chemical reaction, meanwhile the oxidation reaction rate was controlled by the chemical reaction and the diffusion in the product layer. Finally, the kinetic parameters obtained for the selected oxygen carriers were included into a mathematical model to describe the behaviour of these particles in the fuel reactor of a CLC system.

INTRODUCTION

In a chemical-looping combustion (CLC) process, fuel gas (natural gas, syngas, etc.) is burnt in two reactors. In the first one, a metallic oxide that is used as oxygen source is reduced by the feeding gas to a lower oxidation state, being CO_2 and steam the reaction products. In the second reactor, the reduced solid is regenerated with air to the fresh oxide, and the process can be repeated for many successive cycles. CO_2 can be easily recovered from the outlet gas coming from the first reactor by simple steam condensation. Consequently, CLC is a clean process for the combustion of carbon containing fuels preventing the CO_2 emissions to atmosphere. The main drawback of the overall process is that the carriers are subjected to strong chemical and thermal stresses in every cycle and the performance and mechanical strength can decay down to unacceptable levels after enough number of cycles in use.

Different metal oxides have been proposed in the literature [1–3] as possible candidates for CLC process: CuO, CdO, NiO, Mn_2O_3, Fe_2O_3, and CoO. In general, these metal oxides are combined with an inert which acts as a porous support providing a higher surface area for reaction, as a binder for increasing the mechanical strength and attrition resistance, and, additionally, as an ion conductor enhancing the ion permeability in the solid [4,5]. An oxygen carrier in a CLC power plant must show high reaction rate and conversion, resistance against carbon deposition, sufficient durability in successive cycle reactions and high mechanical strength.

The development of oxygen carrier particles have been investigated by the research groups at Tokyo Institute of Technology [4–10], Chalmers University of Technology [11–15], TDA Inc. [16], Consejo Superior de Investigaciones Científicas [17], Korea Institute of Energy Research [18–22], and Politecnico di Milano [23].

Ishida et al. [4–10] have investigated the effect of temperature, particle size, gas composition and pressure on the reduction and oxidation rates and on carbon deposition of Fe, Ni, and Co oxides in a TGA, using H_2, CO, or CH_4 as fuels and air as oxidising gas. The effect of the inert used as a binder and its concentration was also analysed [4]. They concluded that the carbon deposition and the reaction rates and conversions, in addition to the operating conditions used (temperature, particle size, gas composition, total pressure, etc.), depended strongly on the chemical nature of the solid materials [8,9].

Lyngfelt, Mattisson and co-workers [11–13] have investigated the behaviour of different metal oxides, mainly based on iron, using CH_4 and air in fixed-bed and fluidized-bed reactors. They found higher reaction rates and lower particle breakage for synthetic samples as compared with the performance exhibited by natural samples. Recently, these authors [14] prepared NiO, CuO, CoO, and Mn_3O_4 based carriers on alumina support by dry impregnation, and their reactivity was studied in a TGA. They observed that the Ni or Cu containing materials showed high reactivity at all temperatures tested, however, Mn and Co containing carriers showed a rather poor reactivity. Moreover, they have investigated the design of boilers working with CLC process [15].

Copeland et al. [16] developed oxygen carriers to be used in their Sorbent Energy Transfer System (SETS). This system has many elements in common with CLC process; however, SETS uses a thermal neutral reducing reactor versus the CLC endothermic reactor. They prepared oxygen carriers containing Cu, Fe, and Ni with a variety of binder materials and active metal oxide contents. Due to the high temperatures of the SETS reactions, alumina and aluminates were the preferred binders to prepare the carriers. They eliminated Cu as a potential oxygen carrier by agglomeration problems in the fluidized bed (FB), and obtained successfully results with Fe and Ni based carriers.

In this work a significant number of oxygen carriers were prepared and tested in a thermogravimetric analyser (TGA) and in a FB. The best oxygen carriers to be used in a CLC process were selected based on crushing strength, attrition, agglomeration, and reactivity data and its variation during successive reduction–oxidation cycles. For the selected carriers, the kinetic parameters were determined by analysing the operating conditions on their reaction rate.

EXPERIMENTAL/STUDY METHODOLOGY

Preparation of Oxygen Carriers

The oxygen carriers were composed of a metal oxide as an oxygen source for the combustion process, and an inert as a binder for increasing the mechanical strength. In the Grangemouth Capture Project (GRACE), three different preparation methods were used. Consejo Superior de Investigaciones Científicas (CSIC) prepared oxygen carriers by mechanical mixing and by impregnation and Chalmers University of Technology (CUT) prepared oxygen carriers by freeze granulation. The carriers were designated with the chemical symbol referred to the active metal oxide, followed by the weight concentration of active phase used, the symbol for the binder used (Al, alumina; Si, silica; Se, sepiolite; Ti, titania; and Zr, zirconia), the sintering temperature, and finally the preparation method used (M, mechanical mixing; I, impregnation; FG, freeze granulation).

Mechanical mixing

The oxygen carriers were prepared from commercial pure oxides as powders of particle size < 10 μm, being CuO, Fe_2O_3, MnO_2, NiO the active oxides and Al_2O_3, sepiolite ($Mg_4Si_6O_{15}(OH)_2{\cdot}6H_2O$), SiO_2, TiO_2, ZrO_2 the inerts. In addition, graphite as a high-temperature pore forming additive enhancing chemical reaction was also added during preparation.

A powder mixture including the active metal oxide and the inert in the desired concentration, and 10 wt% of graphite, was converted by addition of water into a paste of suitable viscosity to be extruded in a syringe,

obtaining cylindrical extrudates of about 2 mm diameter. These extrudates were softly dried at 80 °C overnight, cut at the desired length, and sintered at different temperatures between 950 and 1300 °C for 6 h in a muffle oven. The extrudates were ground and sieved to obtain the desired particle size.

For screening purposes, materials from all possible combinations between active metal oxides and inerts in three different ratios (40:60, 60:40, and 80:20) and sintered at four temperatures (950, 1100, 1200, and 1300 °C) were prepared. The apparent density of solids varied from 1000 to 5000 kg/m^3 (which corresponded to particle porosities from 0.1 to 0.77) depending on the materials used, the composition of the extrudates, and the sintering temperature. Higher sintering temperatures usually produced oxygen carriers with a higher apparent density and a lower porosity.

Impregnation
Fresh extrudates of inert (SiO_2, TiO_2, etc.) were prepared following the same method described for samples prepared by mechanical mixing. The extrudates were subsequently crushed, ground and sieved into particles of 200–400 μm in size, in order to increase the efficiency of the subsequent impregnation with a saturated aqueous solution of $Cu(NO_3)_2$. The desired active phase loading was achieved by applying successive incipient wet impregnations followed by calcination at 500 °C to decompose the impregnated copper nitrate into insoluble copper oxide.

Crushing Strength Determination
The mechanical strength of the oxygen carriers was determined by using the ASTM D-4179 method. This method allows the measurement of the minimum normal force required to crush a cylindrical extrudate placed between two plates in horizontal position. The crushing strength was obtained dividing the force applied by the extrudate length. The final measure was obtained from the average of at least 15 different measurements undertaken on different extrudates randomly chosen.

Reactivity Tests in a Thermogravimetric Analyser
Reactivity tests of the oxygen carriers were carried out in a TGA system, CI Electronics type, described elsewhere [17]. For the reactivity experiments, the oxygen carrier was loaded in the platinum basket and heated to the set operating temperature in air atmosphere. After stabilisation, the experiment was started by exposing the oxygen carrier to alternating reducing and oxidizing conditions. To avoid mixing of combustible gas and air, nitrogen was introduced for 2 min after each reducing and oxidising period. Some experiments without sample were initially carried out to detect the buoyancy effects due to the change of the reacting gases.

The gases used were CH_4 for reduction and air for oxidation. The reducing gas was saturated in water by bubbling through a water containing saturator at the selected temperature to reach the desired water concentration. The experiments were carried out at temperatures up to 950 °C for the oxygen carriers based on Fe, Mn and Ni, and 800 °C for the oxygen carriers based on Cu, because at higher operating temperatures CuO, although stable in air, decomposed in N_2 atmosphere into Cu_2O with the subsequent loss of oxygen transport capacity of the carrier.

Attrition Tests in Fluidized Bed
Figure 1 shows the experimental set-up used at CSIC for the oxygen carrier testing. It consisted of a system for gas feeding, a FB reactor, a two ways system to recover the solids elutriated from the FB, and a gas analysis system. The gas feeding system had different mass flow controllers connected to an automatic three-way valve. This valve always forced to pass N_2 between the reducing gas and the oxidation gas, to avoid explosions. The FB reactor of 54 mm D.I. and 500 mm height, with a preheating zone just under the distributor, was composed by 300 g of silica sand with a particle size 0.2–0.3 mm. The experiments were carried out by using batches of oxygen carriers of about 50 g with a particle size 0.1–0.2 mm. The entire system was inside an electrically heated furnace. Downstream from the FB there was two hot filters to recover the solids elutriated from the bed during the successive reduction–oxidation cycles, which allowed to obtain elutriation data at different times or number of cycles. The gas composition at each time was continuously measured by different gas analysers. The H_2O, CO, CO_2 and CH_4 were determined in an infrared analyser, the O_2 in a paramagnetic analyser, and the H_2 by gas conductivity.

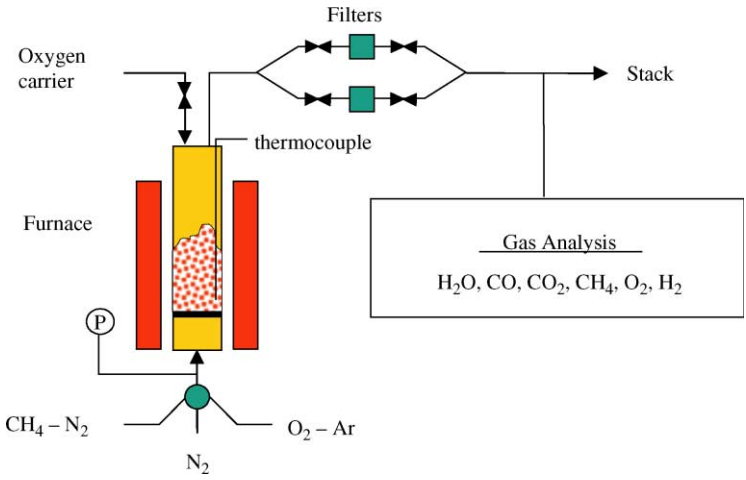

Figure 1: Experimental set-up for attrition determination during multicycle tests in FB.

Due to the increase of the gas velocity produced during the CH_4 conversion, the inlet superficial gas velocity (15 cm/s) and the composition of the reducing gas (50% CH_4:50% N_2) were selected to avoid exceed the terminal velocity of the particles. In addition, because the heat produced during the oxidation period, a gas mixture (15 cm/s) with 8% O_2 in Ar was used instead of air to avoid a large temperature increase. The set-point temperature was 950 °C for the oxygen carriers based on Fe, Mn and Ni, and 800 °C for the oxygen carriers based on Cu.

RESULTS AND DISCUSSION

Mechanical Strength

The crushing strength was highly dependent on the type of active metal oxide and its concentration, the inert used as a binder, and the sintering temperature [17]. A higher sintering temperature increased the crushing strength of the oxygen carriers although this temperature was limited for some carriers by the decomposition or melting of the involved compounds. This effect was especially important in the Cu and Mn oxygen carriers, and in those using sepiolite as inert. On the other hand, there was not a clear correlation between crushing strength and active metal oxide content.

Cu-based oxygen carriers only showed a measurable crushing strength when using SiO_2 and TiO_2 as inerts. Fe-based oxygen carriers showed high crushing strength values, specially those prepared with Al_2O_3, TiO_2 and ZrO_2 and sintered at temperatures above 1100 °C. Mn-based oxygen carriers only had high crushing strengths when using SiO_2 or TiO_2 sintered at 1100 °C, and ZrO_2 sintered at temperatures higher than 1100 °C. Ni-based oxygen carriers showed in general terms a low crushing strength excepting when using SiO_2 or TiO_2 as inerts.

Reactivity of Oxygen Carriers

TGA experiments allowed to analyse the reactivity of the oxygen carriers under well-defined conditions, and in the absence of complex fluidizing factors such as those derived from particle attrition and inter-phase mass transfer processes. For screening purposes, five cycles of reduction (70% CH_4:30% H_2O) and oxidation (100% air) were carried out at 800 °C for Cu and 950 °C for Fe, Mn, and Ni carriers. The carriers usually stabilized after the first cycle, for which the reduction reaction rate was slower. The oxygen carrier reactivity corresponding to the cycle 5 was used for comparison purposes.

Reactivity data were obtained in TGA tests from the weight variations during the reduction and oxidation cycles as a function of time. To convert weight data into carrier conversions a description of the involved chemical reactions was necessary. On the basis of thermodynamics the reactions involved for the different oxygen carriers are given in Table 1.

TABLE 1
REACTIONS AND OXYGEN TRANSPORT CAPACITY FOR THE OXYGEN CARRIERS IN CLC

	R_0	b	Z
Copper			
$CH_4 + 4CuO \rightarrow CO_2 + 2H_2O + 4Cu$	0.201	4	0.56
$4Cu + 2O_2 \rightarrow 4CuO$		2	1.77
Iron			
$CH_4 + 12Fe_2O_3 \rightarrow CO_2 + 2H_2O + 8Fe_3O_4$	0.033	12	0.98
$8Fe_3O_4 + 2O_2 \rightarrow 12Fe_2O_3$		4	1.02
$CH_4 + 4Fe_2O_3 \rightarrow CO_2 + 2H_2O + 8FeO$	0.100	4	0.83
$8FeO + 2O_2 \rightarrow 4Fe_2O_3$		4	1.21
$CH_4 + 4/3Fe_2O_3 \rightarrow CO_2 + 2H_2O + 8/3Fe$	1.000	4/3	0.47
$8/3Fe + 2O_2 \rightarrow 4/3Fe_2O_3$		4/3	2.14
Manganese			
$CH_4 + 4Mn_3O_4 \rightarrow CO_2 + 2H_2O + 12MnO$	0.070	4	0.83
$12MnO + 2O_2 \rightarrow 4Mn_3O_4$		6	1.20
Nickel			
$CH_4 + 4NiO \rightarrow CO_2 + 2H_2O + 4Ni$	0.214	4	0.59
$4Ni + 2O_2 \rightarrow 4NiO$		2	1.70

The oxygen transport capacity, R_0, for the respective active metal oxide can be defined by the oxygen content ratio in the reduced, m_{red}, and oxidized, m_{ox}, forms through the expression:

$$R_0 = \frac{m_{ox} - m_{red}}{m_{ox}}$$

Table 1 shows the oxygen transport capacity for the different oxygen carriers derived from the above reactions. The maximum oxygen transport capacity corresponded to the oxygen carriers based on Cu and Ni. However, the transport capacity of the carrier obviously decreased due to the presence of the inert.

For Fe-based carriers prepared with Fe_2O_3 as active metal oxide, different reactions are possible, which correspond to the transformations Fe_2O_3–Fe_3O_4, Fe_2O_3–FeO, or Fe_2O_3–Fe. The oxygen transport capacity of the carriers is highly dependent on the reaction considered being for the reaction Fe_2O_3–Fe three times higher than for the reaction Fe_2O_3–FeO and for this reaction three times higher than for the reaction Fe_2O_3–Fe_3O_4. The stable iron species are dependent on the reducing gas composition and temperature. In this work, the weight variations observed in the reactivity tests were mainly associated with the transformation Fe_2O_3–FeO.

Figure 2 shows examples of the reactivity data obtained in TGA, both in the reduction and the oxidation reactions, for some oxygen carriers based on Fe, Mn, and Ni as a function of sintering temperature. In general, an increase of the sintering temperature produced a decrease in the reaction rate. The curves corresponding to the reduction of the NiO were plotted until the formation of carbon was important.

Table 2 gives a summary of the reactivity data for all the oxygen carriers prepared at CSIC by mechanical mixing, and Figure 3 shows an example of the notation used in the table. Cu-based oxygen carriers sintered at 950 °C exhibited a high reactivity with reaction times for complete reduction lower than 1 min. The oxidation conversions at 1 min of reaction varied from 80 to 100%. In some cases, the final oxidation rate

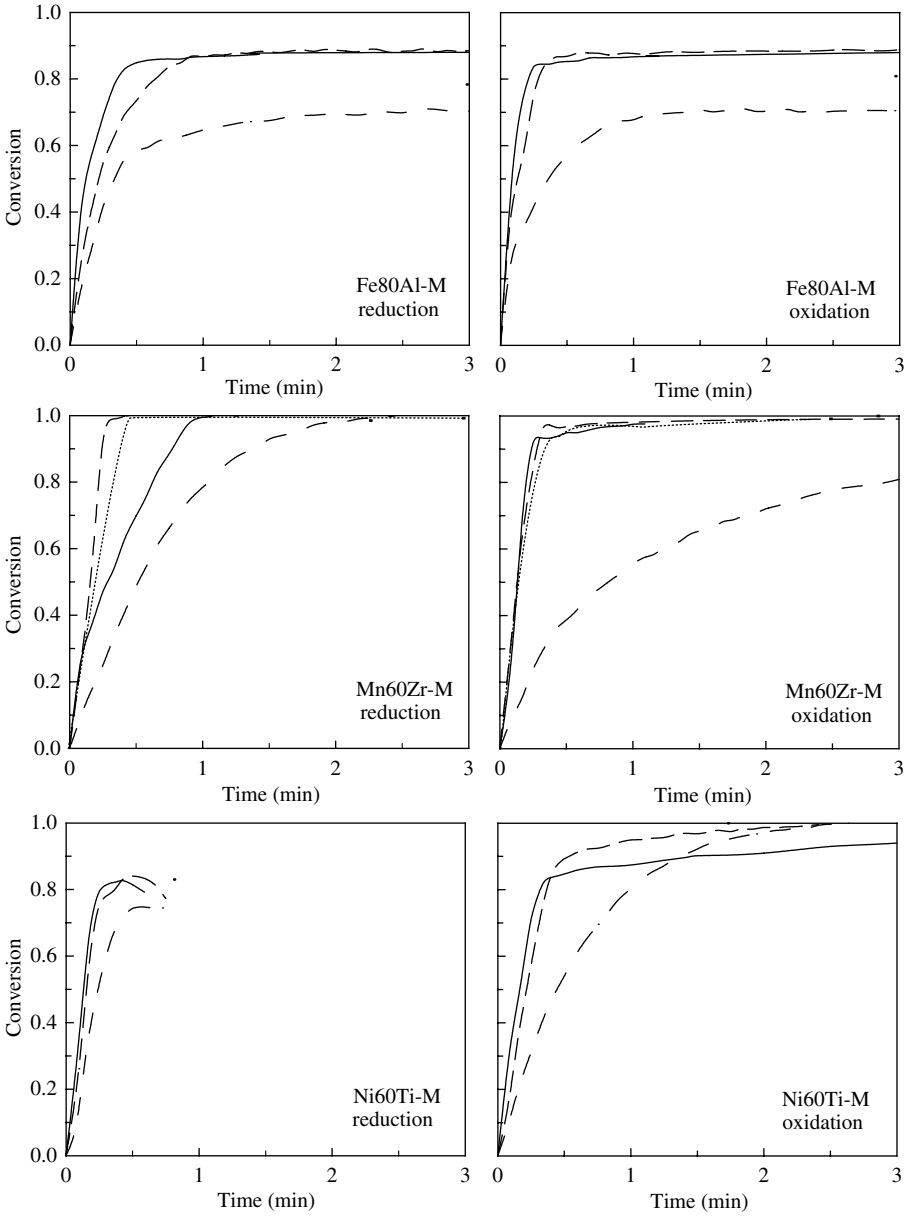

Figure 2: Examples of reactivity of oxygen carriers prepared by mechanical mixing and extrusion during reduction and oxidation as a function of the sintering temperature. (— 950 °C, — —1100 °C, ·····1200 °C, –··– 1300 °C.

was substantially lower, probably, by diffusional effects inside the extrudates. Fe-based oxygen carriers exhibited a high reactivity during reduction and oxidation, although the reduction to FeO was not complete in most of the cases. The Mn-based oxygen carriers showed a different behaviour depending on the active metal oxide content, the type of inert, and the sintering temperature. The best performance was obtained using ZrO_2 as inert. Ni-based oxygen carriers exhibited a very high reactivity during reduction with reaction times lower than 30 sec for complete conversion. The behaviour during the oxidation process was highly dependent on the oxygen carrier considered. The best performance was obtained with Ni–Ti carriers, which exhibited high reactivity both in the reduction and the oxidation processes.

Screening of Oxygen Carriers

A preliminary screening of the most suitable carrier to be used in a CLC process was made based on the decomposition or melting point of the carriers, crushing strength data, and reactivity tests in TGA. Fresh extrudates with crushing strengths below 10 N/mm were considered exceedingly soft and rejected. Other oxygen carriers exhibiting very low reactivity due to the formation of inactive compounds by a solid/solid reaction (Mn40Ti) or excessive thermal sintering (Ni80Se1300) were also rejected. Considering the above criteria, Table 2 shows the best oxygen carriers to be further used in CLC systems. That includes carriers prepared with SiO_2 or TiO_2 as inert and sintered at 950 °C as the best Cu-based oxygen carriers. Fe-based oxygen carriers prepared with all inerts can be considered potentially suitable for CLC systems although some of them must be prepared at some specific conditions. Those prepared with Al_2O_3 and ZrO_2 as inerts showed the best behaviour. ZrO_2 was the best inert for preparing Mn-based oxygen carriers, and TiO_2 for preparing Ni-based oxygen carriers. Other carriers, as Fe–Ti sintered at 1200 and 1300 °C, and Ni–Si, exhibited an acceptable crushing strength but they did not have a high reactivity.

Multicycle testing in TGA

In every cycle the carrier undergoes important chemical and structural changes at high operating temperature and, consequently, it is expected substantial changes in performance of the carriers with the number of cycles. The oxygen carriers exhibiting acceptable crushing strengths and high conversions and reactivities were selected for 100-cycles testing in successive oxidation–reduction tests in TGA. Figure 4 shows the reactivity of the sample Cu40Si950-M in several selected cycles for reduction and oxidation. The curves were almost coincident revealing that the carrier reactivity was not affected substantially by the number of cycles in use. Similar results were observed with other carriers prepared by mechanical mixing. However, with the carriers Cu–Si, Cu–Ti, Ni–Ti, and those prepared with a MeO:inert ratio of 80:20, the original cylindrical shape of the fresh extrudates was completely converted in an amorphous powder pile after reaction indicating that the mechanical strength of the carrier was severely affected. From these multicycle tests, it was concluded that the oxygen carriers prepared by mechanical mixing exhibited high reactivity and excellent chemical stability but some of them poor mechanical strength. Consequently, the method of preparation of the Cu and Ni-based oxygen carriers must be improved to decrease the unacceptable rapid degradation of their mechanical properties as the number of cycles increased.

The effects of the accumulative chemical and thermal stresses in every cycle could be minimized if MeO as active phase is retained by impregnation within the porous texture of an inert support. In this case, the inert support could be sintered at higher temperature to increase substantially its mechanical strength. In this work, samples of titania, alumina and silica impregnated with CuO were prepared following the conventional method above described. These carriers showed good chemical stabilities and high reactivities, similar to or even higher than those prepared by mechanical mixing. Crush strength measurements revealed that the mechanical properties of the fresh carriers were preserved after reaction in multicycle tests, and the presence of holes or cracks were not evidenced in SEM micrographs of surfaces of the fresh and after-use carriers. These results suggested that oxygen carriers prepared by impregnation on rigid and porous supports were potential candidates for CLC process. Also, CUT prepared a Ni-based oxygen carrier by freeze granulation, Ni_{CUT}-FG, to be tested in their CLC pilot plant [25]. This carrier showed a good chemical stability and mechanical strenght and a very high reactivity in the multicycle testing in TGA.

Multicycle testing in FB

To improve the screening it was necessary to know the behaviour of the most promising carriers during successive reduction–oxidation cycles in a FB, which considered both the structural changes as a

TABLE 2
REACTIVITY OF OXYGEN CARRIERS AND PRELIMINARY SCREENING

		Metal-based oxygen carriers															
		Cu				Fe				Mn				Ni			
	T_{sint} (°C)	950	1100	1200	1300	950	1100	1200	1300	950	1100	1200	1300	950	1100	1200	1300
Inert	MeO(%)	red-oxid															
Al_2O_3	80	a-a	e-e			a-a	**a-a**	**b-b**	**b-b**	a-a	b-b	e-e		a-a	a-b*	a-b*	b-c*
	60	a-a	e-e			a-a	**b-b**	**b-b**	**b-b**	b-b	c-c	e-e		a-a	a-b*	b-c*	e-e
	40	a-a	e-e			a-a	**a-a**	**b-b**	**b-b**	c-c	e-e	e-e		a-a	b-c	c-c	e-e
Sepiolite	80	a-a				a-a	**a-a**			a-a	a-a			a-a	a-a	a-a	e-e
	60	a-a				a-a	**a-a**			a-a	a-a			a-a	a-a	b-b	
	40	a-a				a-a	**a-a**			a-a	c-e			a-a	b*-a	e-e	
SiO_2	80	**a-a**				**b-b**	**b-b**			**a-a**	**b-b**			a-c*	a-c*	a-c*	a-b*
	60	**a-a**				**a-a**	**b-b**			**a-a**	e-e			a-c*	**a-d**	**a-d**	**a-c**
	40	**a-a**				**a-a**	**a-a**			**a-a**	e-e			**a-c***	**b-d**	**b-d**	
TiO_2	80	**a-a**				**a-a**	**b-b**	**b-c***	**b-c***	b-b	**b-b**			a-b*	**a-b***	**a-b***	**b*-c***
	60	**a-a**				**a-a**	**b-b**	**b-c***	**c-c**	e-e	e-e			**a-a**	**a-a**	**a-a**	**a-b***
	40	**a-a**				**a-a**	**b-c***	**b-c***	**b-d**	e-e	e-e			**a-a**	**a-a**	**a-a**	**a-b***
ZrO_2	80	a-a				a-a	**a-a**	**a-a**	**b-b**	a-a	**a-a**	**a-a**	**a-b***	a-c*	a-c*	a-d	a-d
	60	a-a				**a-a**	**a-a**	**a-a**	**b-b**	a-a	**a-a**	**a-a**	**a-b***	a-b*	a-b*	a-b*	a-b*
	40	a-a				**a-a**	**a-a**	**a-a**	**b-b**	a-a	**a-a**	**a-a**	**b*-b***	a-b*	a-b*	a-b*	a-b*

Melt or decompose

Low reactivity and crushing strength

Selected particles by mechanical strength and reactivity

* Denotes extension of curve b and c along the dashed curves in Figure 3.

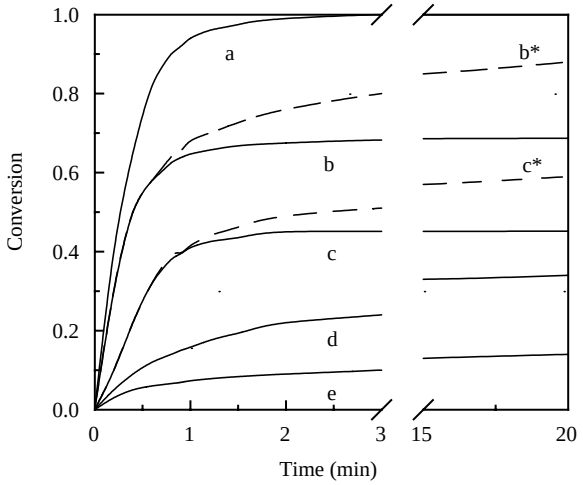

Figure 3: Typical conversion curves obtained during reactivity testing, and used for notation in Table 2.

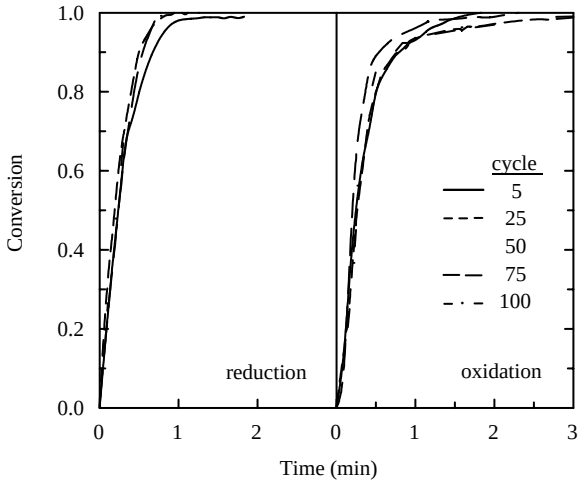

Figure 4: Reactivity of the oxygen carrier Cu40Si950-M during multicycle tests in TGA.

consequence of the chemical reaction, and the attrition phenomena existing in a FB, as well as the possible agglomeration of the solids. Figure 5 shows the attrition rate measured with some oxygen carriers prepared by mechanical mixing, impregnation, and freeze granulation that were selected because of their good behaviour in the TGA tests. The attrition rates were usually high in the first cycles due to the rounding effects on the particles and as a consequence of the fines sticked to the particles during preparation (grinding + sieving). Later, the attrition rates due to the internal changes produced in the particles by the successive reduction and oxidation processes, decreased.

It was also observed that Cu-based carriers prepared by mechanical mixing (Cu40Si950-M) showed agglomeration in the FB tests, however, this problem was not observed with the Cu-based carriers prepared by impregnation (CuTi-I, CuAl-I). It was concluded that the use of Cu-based oxygen carriers in a CLC system was restricted to the particles prepared by impregnation. The MnZr-M carriers showed agglomeration and most of the particles were sticked to the wall of the reactor. Finally, the Ni-based oxygen carriers (Ni_{CUT}-FG) and the Fe-based oxygen carriers (FeAl-M) did not agglomerate and showed low attrition rates, as it can be seen in Figure 5.

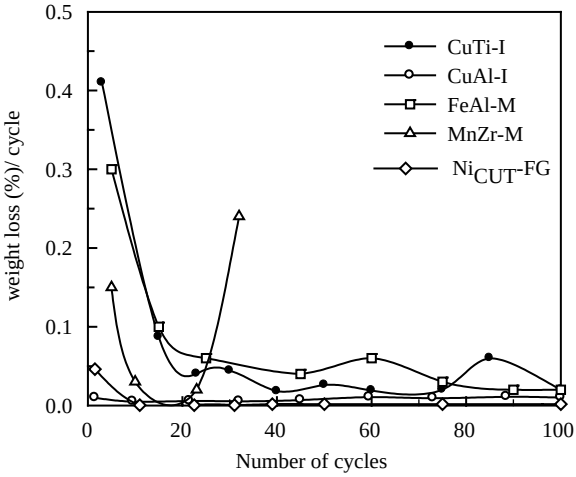

Figure 5: Attrition rates of the oxygen carriers in FB.

After the FB tests carried out at CSIC and CUT, three kinds of oxygen carriers were selected and prepared to be tested in the CLC pilot plant [24]: Cu_{CSIC}-I, Fe_{CUT},FG, and Ni_{CUT}-FG.

Kinetic of Reduction and Oxidation Reactions

The effect of the main operating variables (temperature, gas concentration, gas products, etc.), on the reduction and oxidation rates were analysed by TGA to determine the kinetic parameters of the selected carriers. The changing grain size model proposed by Georgakis et al. [25] was adapted to the specific case of the reduction and oxidation reactions taking place in CLC. This model considers the particles composed of grains with an initial radius r_0. As the reaction proceeds, the grain size changes as a consequence of the different molar volumes of the product with respect to the reactant, following a shrinking core model scheme. Table 2 gives the values of the stoichiometric coefficients, b, and the expansion ratio, Z, for the different reactions. Considering negligible the resistances to gas film mass transfer and diffusion inside the particle, as previously determined, the equations that describe this model depending on the resistances controlling the reaction are given in Table 3.

The heat generated during the exothermic reactions could increase the temperature of the particle, and produce the melting or sintering of the metal reactants or products. Moreover, it could affect to the reaction rates observed, and to the validity of the kinetic parameters determined. To know the temperature variations produced inside the oxygen carrier particles during the exothermic reactions taking place during oxidation in a FB, a heat balance was added to the particle reaction model. The effect on the particle temperature of the oxygen carrier type, particle size, oxygen concentration and fraction of metal oxide present in the carrier was analysed.

The highest exothermic reaction of all the reactions considered corresponds to the Ni oxidation. Figure 6 shows the variation with time of the mean temperature and conversion of carrier particles for different particle

TABLE 3
KINETIC EQUATIONS FOR THE CHANGING GRAIN SIZE MODEL USED FOR CLC REACTIONS

Chemical reaction	
$\frac{t_c}{\tau_c} = 1 - (1 - X)^{1/3}$	$\tau_c = \frac{\rho_m r_0}{b k_1 C^{n_1}(1 + k_2 C_{H_2O}^{n_2})}$
	$k_1 = k_{1,0} e^{(-E_1/RT)}$
	$k_2 = k_{2,0} e^{(-E_2/RT)}$
Diffusion in the product layer	
$\frac{t_d}{\tau_d} = 3 \cdot \left[1 - (1 - X)^{2/3} + \frac{1 - [Z + (1 - Z)(1 - X)]^{2/3}}{Z - 1}\right]$	$\tau_d = \frac{\rho_m r_0^2}{6 b D_e C}$
	$D_e = D_{e,0} e^{-k_x X}$
	$D_{e,0} = D_{e,0,0} e^{(-E_3/RT)}$
	$k_x = k_{x,0} e^{(-E_4/RT)}$

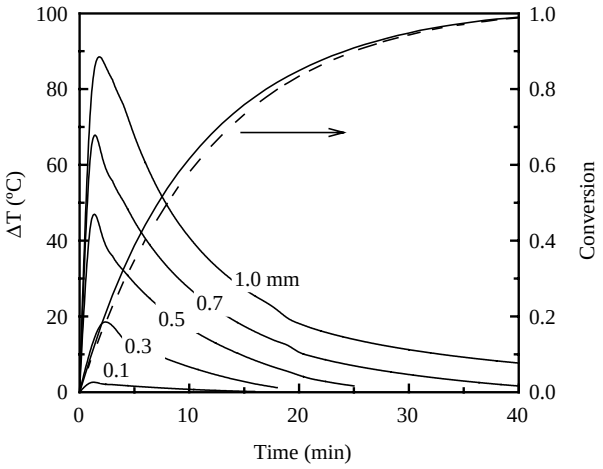

Figure 6: Temperature variation in the particle during the oxidation of Ni-based oxygen carriers (— with heat balance, - - - isothermal particle, $dp = 0.7$ mm, 950 ºC.

sizes in the oxidation of Ni to NiO. The mean temperature of the particles quickly increased up to a maximum and smoothly decreased until reach the bed temperature. These temperature increases were small and did not affect the reaction rate. Almost identical curves of conversion with time were achieved considering the heat balance and assuming isothermal particles, as showed in the Figure for the 0.7 mm particles.

Figure 7 shows the maximum variation of temperature reached during the oxidation and reduction reactions with different oxygen carriers. The maximum temperature variations were reached during the Ni oxidation with values of about 90 ºC for 1 mm particles. However, maximum variations of 20 ºC were reached for particles under 0.3 mm. Therefore, the particles can be considered isothermal for most of the reactions when using small particle sizes, as it would be normal in a CLC process.

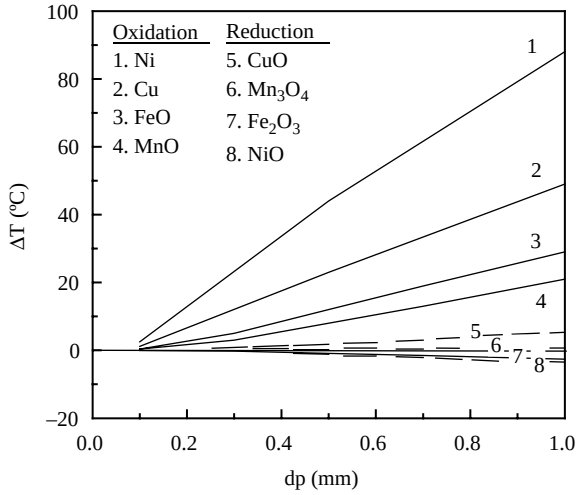

Figure 7: Maximum variation of temperature as a function of particle size for different oxygen carriers and reactions (— oxidation, - - - - reduction).

Assuming isothermal particles, the reaction model was used to determine the kinetic parameters of the different reactions for each oxygen carrier. Table 4 shows the physical properties of the selected oxygen carriers and Table 5 shows the kinetic parameters determined. It was found that the reduction reaction of the oxygen carriers with CH_4 was controlled by the chemical reaction, and the three oxygen carriers exhibited high reaction rates under the typical operating conditions of a CLC system. Figure 8 shows the effect of the CH_4 concentration for the three oxygen carriers. An increase in the CH_4 concentration produced and increase in the reduction rate. However, since during the reduction of the oxygen carriers in the fuel reactor the CH_4 is mixed with the gases produced in the reaction, H_2O and CO_2, the effect of these gases was analysed. The CO_2 concentration did not affect the reduction reaction rate for any oxygen carrier. At opposite, the H_2O strongly affected the reduction reaction rate (a new parameter to consider their effect was introduced in the equation of the complete conversion time, as can be observed in Table 3). This effect was different depending on the carrier. The H_2O accelerated the reduction reaction rate of the Cu-based oxygen carrier with CH_4, as it can be observed in Figure 9. Oppositely, the presence of H_2O decreased the reaction rate for the Fe-based oxygen carriers, which produced a negative value of the kinetic parameter k_2. For the

TABLE 4
PHYSICAL PROPERTIES OF THE SELECTED OXYGEN CARRIERS

	Cu_{CSIC}-I	**Fe_{CUT}-FG**	**Ni_{CUT}-FG**
Porosity	0.3	0.3	0.36
Specific surface area BET (m^2/g)	1.1	2.5	0.8
Particle size, dp (mm)	0.24	0.15	0.23
Grain radius of MeO, r_0 (m)	0.6×10^{-6}	0.26×10^{-6}	0.69×10^{-6}
Grain radius of Me, r_0 (m)	0.5×10^{-6}	0.24×10^{-6} [a]	0.58×10^{-6}
Molar density of MeO, ρ_m (mol/m^3)	80402	32811	89290
Molar density of Me, ρ_m (mol/m^3)	140252	79277[a]	151618

[a] Assuming Me = FeO.

TABLE 5
KINETIC PARAMETERS DETERMINED FOR THE SELECTED OXYGEN CARRIERS

	Cu_{CSIC}-I	Fe_{CUT}-FG	Ni_{CUT}-FG
Reduction reaction			
$k_{1,0}$ (m/s)(mol/m^3)$^{1-n1}$	4.1×10^{7}	1.6×10^{-2}	0.7
E_1 (kJ/mol)	257	56	78
n_1	0.8	0.3	0.8
$k_{2,0}$ (m^3/mol)	2.7×10^{-4}	-10	
E_2 (kJ/mol)	-60	44	
n_2	2	1	
Oxidation reaction			
$k_{1,0}$ (m/s)(mol/m^3)$^{1-n1}$	1.1×10^{-2}	7.8×10^{-5}	1.1×10^{-2}
E_1 (kJ/mol)	27	7	26
n_1	1	1	0.3
$D_{e,0,0}$ (m^2/s)	6.7×10^{15}	6.5×10^{-8}	
E_3 (kJ/mol)	420	0	
$k_{x,0}$ ($-$)	242	18	
E_4 (kJ/mol)	25	0	

Ni-based carriers, the H_2O was necessary to avoid the carbon formation, and it was not possible to detect their effect on the reaction rate of the NiO with CH_4.

Figure 10 shows the effect of the oxygen concentration during the oxidation of the three oxygen carriers. The three materials exhibited a high reactivity, even at low oxygen concentrations, with reaction times for a 90% of conversion lower than 1 min. The values of the kinetic parameters of the oxidation reaction were obtained by fitting of the experimental conversion-time curves, assuming in the reaction a mixed control of the chemical reaction and the diffusion in the product layer. For the Cu and Fe carriers, a satisfactory fit was obtained assuming the product layer diffusion coefficient to be a function of the conversion, and not a constant as in the original grain model (see Table 3). The problems of carbon formation found during the

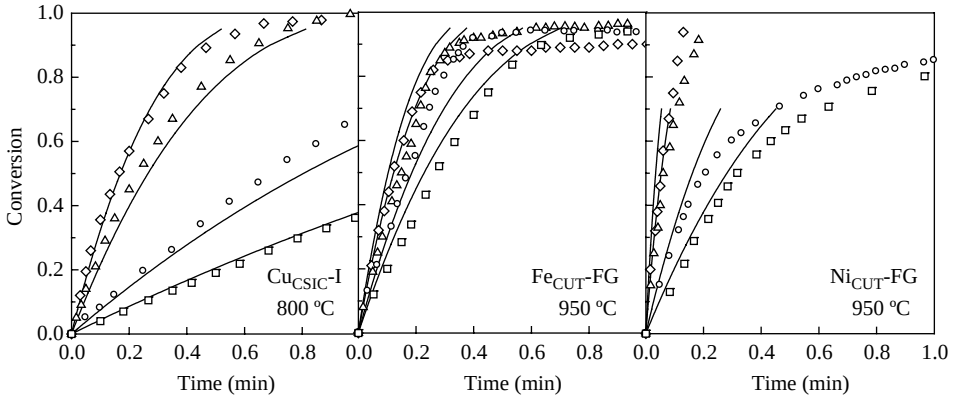

Figure 8: Effect of CH_4 concentration on the reduction rate of the selected oxygen carriers. Continuous line = model predictions. CH_4 concentration: □ 5%, ○ 10%, **Δ** 40%, ◇ 70%.

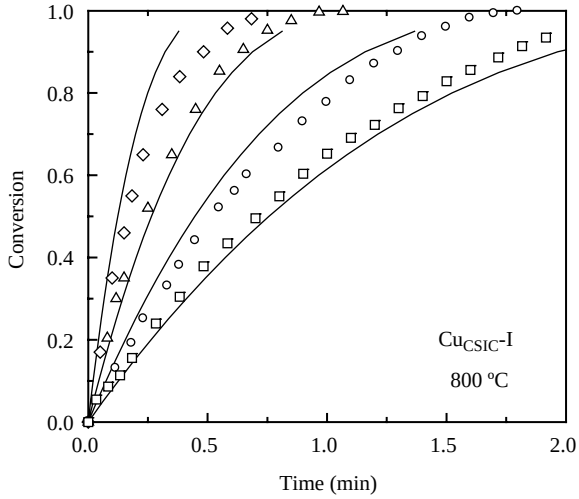

Figure 9: Effect of H_2O concentration on the reduction rate of Cu_{CSIC}-I oxygen carrier. Continuous line = model predictions. H_2O concentration: □ 10%, ○ 20%, **Δ** 30%, ◇ 48%.

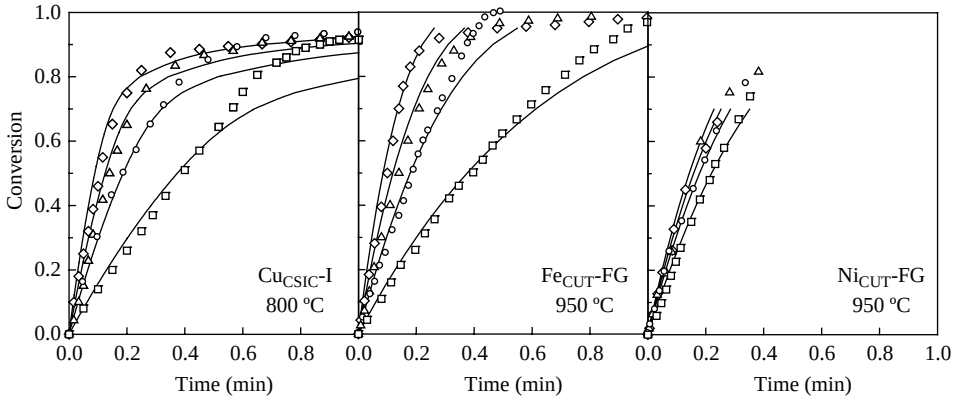

Figure 10: Effect of O_2 concentration on the oxidation rate of the selected oxygen carriers. Continuous line = model predictions. O_2 concentration: □ 5%, ○ 10%, **Δ** 15%, ◇ 21%.

reduction of the Ni oxygen carriers made impossible to determine the diffusion through the product layer with accuracy since no complete reduction of this oxygen carrier could be assured. In this case, apparent kinetic parameters of the oxidation reaction were obtained for the first instants of the reaction, assuming that the oxidation was controlled by the chemical reaction.

Mathematical Modelling of the Fuel Reactor

A mathematical model for a bubbling FB fuel reactor previously developed [26] was used together the reaction kinetics previously determined to optimize the performance of this reactor in CLC systems. The model considered both the hydrodynamic of the FB (dense bed and freeboard) and the kinetics of each oxygen carrier reduction.

The bed was considered divided in two regions, bubble and emulsion, with plug flow of gas in each region and a gas exchange between both phases [27]. Differential mass balances in the emulsion and bubble phases were made to know the CH_4 and other gas concentrations through the bed height. During CH_4 conversion in CLC systems there is an important gas expansion as a consequence of the reaction stoichiometry. In this case, 1 mol of CO_2 and 2 mol of H_2O are produced per mole of CH_4 consumed. This produces high velocities at the top of the bubbling FB and much solid may be present in the freeboard. As a consequence, a significant extent of the gas conversion may occur there. In this work, the freeboard model proposed by Kunii and Levenspiel [27] was used. In the fuel reactor of a CLC system working with Ni and Fe carriers, in addition to the reaction of the CH_4 with the metal oxide, other gas phase reactions are possible as the methane-reforming reactions with H_2O and CO_2 and the shift reaction. For the reactor modelling, it has been considered that the gas species CH_4, CO_2, H_2O, CO, and H_2 reached the thermodynamic equilibrium in the emulsion zone of the dense bed and in the freeboard.

A simulation of the fuel reactor behaviour can be useful to set up the best operating conditions and optimize the process. The effect of different design and operating variables as the bed height, the oxygen-fuel ratio, and the gas throughput were analysed for each oxygen carrier of Cu, Fe and Ni. For some carriers, as the based on Fe and Ni, the solids fed coming from the oxidation reactor will be determined by the heat balance in the whole CLC process. In these cases, high recirculation solid flows are necessary to maintain the temperature in the fuel reactor because the reduction reactions of these metals with CH_4 are endothermic. An excess of solids, $\gamma = 4$ for Ni and $\gamma = 2.5$ for Fe, is necessary to maintain the heat balance in the system for a temperature difference between the oxidation and fuel reactors of 70 °C, if heat losses are not considered. However, for the oxygen carriers based on Cu, where the reduction reaction is exothermic, the solids flow fed to the fuel reactor will be based on other criteria, mainly on the amount necessary to obtain high CH_4 conversions. Figure 11 shows the effect of the oxygen carrier to fuel ratio, γ, on gas and solid conversion. An increase in the solids feed in produced a higher CH_4 conversion, although the increase for values of γ higher than 1.5 for the Cu-based oxygen carriers produced the complete conversion of the fuel.

Figure 12 show the gas concentration and conversion profiles as a function of the reactor height working with a Ni-based oxygen carrier. Complete CH_4 conversion was obtained, however, it was not possible to reach a complete gas utilisation because some CO (0.4%) and H_2 (0.5%) was present at the gas exit. This values corresponded to the thermodynamic equilibrium values at the operating conditions simulated.

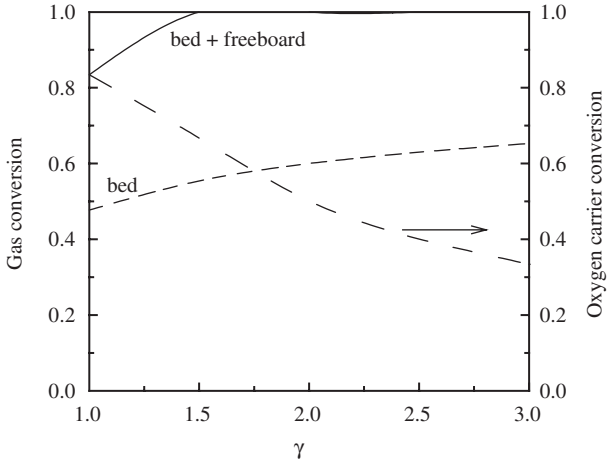

Figure 11: Effect of the excess of a Cu-based oxygen carrier on the gas and carrier conversions. $dp = 0.25$ mm, $T = 800$ °C, $u_0 = 0.5$ m/s, $h_{bed} = 0.5$ m.

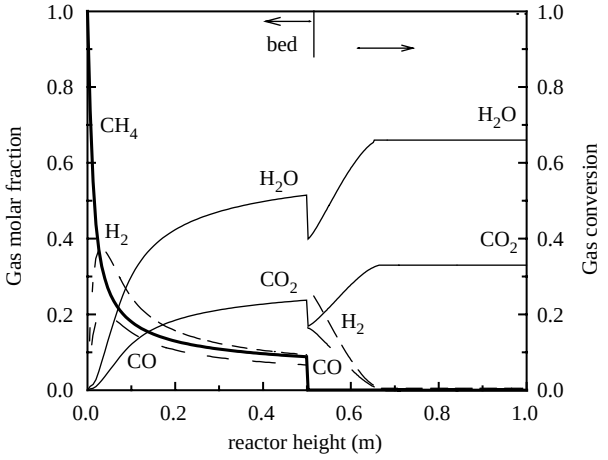

Figure 12: Longitudinal profiles of gas in the fuel reactor for a Ni-based oxygen carrier ($dp = 0.25$ mm, $T = 950$ °C, $\gamma = 4$, $u_0 = 0.5$ m/s, $h_f = 0.5$ m).

The gas throughput of the reactor is directly related with the gas velocity at the inlet, for a given reactor area. In the simulation, a superficial gas velocity of 0.5 m/s at the bottom of the reactor was used, which corresponded to a 4.0 MW_t per square meter of reactor cross section at 950 °C. At industrial scale, higher velocities would be used in the fuel reactor to allow a higher gas throughput per square meter of bed. This will produce the entrainment of the particles in the bed that could be captured by an internal cyclone and returned to the bed. This situation is somewhat different to the used in the reactor modelling here developed,

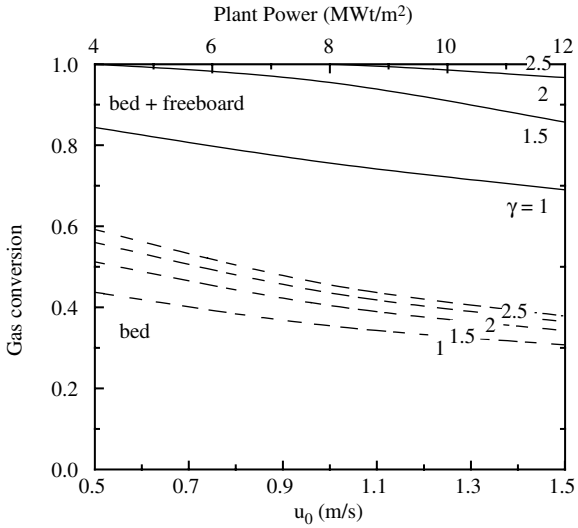

Figure 13: Effect of gas velocity on the CH_4 conversion for a Fe-based oxygen carrier ($dp = 0.25$ mm, $T = 950$ °C, $h_{bed} = 0.5$ m, $h_f = 0.5$ m).

especially with respect to the hydrodynamic behaviour, but a first approach was made with this model. Figure 13 shows the effect of the gas velocity at the inlet of the reactor on the CH_4 conversion working with a Fe-based oxygen carrier and different excess of solids. Higher velocities at the bottom produced an important decrease in the gas conversion obtained in the bubbling bed. This was due to the lower residence time of the particles in the bed as a consequence of the higher bed expansion. This effect was compensated, in some way, with a higher conversion in the freeboard due to a better gas/solid contact in this zone.

The simulation carried out with the selected oxygen carriers based on Cu, Fe, and Ni showed that the three particles are suitable to carry out the CLC process with high performance. The use of one or other carrier will be based on other aspects as the life of the carrier, cost and environmental considerations.

CONCLUSIONS

The effects of the chemical nature and composition of 240 samples of oxygen carriers composed up to 80% of Cu, Fe, Ni, Mn oxides and different inerts prepared by mechanical mixing as cilindrical extrudates were investigated by analysis of the reactivity tests in TGA and mechanical strength data. Based on these properties, Cu-based oxygen carriers prepared using SiO_2 or TiO_2 as inert, Fe-based oxygen carriers prepared with Al_2O_3 and ZrO_2 as inerts, Mn-based oxygen carriers with ZrO_2, and Ni-based oxygen carriers with TiO_2 as inert were the most promising carriers to be used in a CLC system. These best oxygen carriers were tested during 100 successive oxidation–reduction cycles in a TGA and in a FB. The oxygen carriers exhibited high reactivity and excellent chemical stability during multicycle tests, but the mechanical properties of Cu and Ni-based carriers prepared by mechanical mixing were severely affected. To minimize the effects of the accumulative chemical and thermal stresses, other preparation methods must be used. New Cu-based oxygen carriers prepared by impregnation exhibited very high reactivities and complete solid conversions. In addition, they maintained the chemical and mechanical properties of the fresh carriers during FB multicycle tests and did not undergo agglomeration. Ni-based particles prepared at CUT by freeze-granulation also showed high reactivity, good chemical stability and low attrition rates in the FB multicycle tests. Based on the multicycle tests carried out at CSIC and CUT, three kinds of oxygen carriers were selected to be tested in a CLC pilot plant: Cu_{CSIC}-I, Fe_{CUT}-FG, and Ni_{CUT}-FG.

The kinetic parameters of these selected carriers were determined in a TGA. The reduction reaction rate of the oxygen carriers with CH_4 was controlled by the chemical reaction, meanwhile the oxidation reaction rate was controlled by the chemical reaction and the diffusion in the product layer. A heat balance in the particle showed that the particles can be considered isothermal when using small particle sizes, as it would be normal in a CLC process. An increase in the CH_4 concentration produced and increase in the reduction rate, and an important effect of the H_2O was found for this reaction. The H_2O accelerates the reduction reaction rate of the Cu-based oxygen carriers, but decreased the reaction rate of the Fe-based particles. For the Ni-based particles, the H_2O avoided the carbon formation although their effect on the reaction rate could not be determined.

Finally, a simulation carried out with the three selected oxygen carriers showed that it is possible to reach complete CH_4 conversion using a bubbling fluidized with low pressure drop for the fuel reactor. Only with Ni carriers there was an small decrease in the recoverable energy due to the presence of small concentrations of CO and H_2 at the gas outlet by thermodynamic restrictions. The three selected oxygen carriers based on Cu, Fe and Ni are suitable to carry out the Chemical-Looping Combustion process with high performance. The use of one or other carrier will be based on the life of the carrier, cost and environmental considerations.

RECOMMENDATIONS

- To optimize the preparation method of the oxygen carriers to reduce costs, and to improve the carrier formulations to reduce CO and H_2 concentrations at the outlet of the fuel reactor.
- To analyse the behaviour of oxygen carriers under industrial gas stream conditions, including heavy hydrocarbons and sulphur compounds.
- To analyse the performance of the individual fuel and oxidation reactors under different operating conditions, in order to optimize the Chemical-Looping Combustion process.

ACKNOWLEDGEMENTS

This chapter is based on the work in the frame of the GRACE (Grangemouth Capture Project) Project, coordinated by British Petroleum and funded by the EU (ENK5-CT-2001-00571) and by the CCP (CO_2 Capture Project).

REFERENCES

1. H. Ritcher, K. Knoche, *ACS Symp. Ser.* **235** (1983) 71–85.
2. M. Ishida, D. Zheng, T. Akehata, *Energy Int. J.* **12** (1987) 147–154.
3. T. Mattisson, A. Lyngfelt, Capture of CO_2 Using Chemical-Looping Combustion, Scandinavian-Nordic Section of Combustion Institute, 2001.
4. M. Ishida, H. Jin, *J. Chem. Eng. Jpn* **27** (1994) 296–301.
5. M. Ishida, H. Jin, *Ind. Eng. Chem. Res.* **35** (1996) 2469–2472.
6. M. Ishida, H. Jin, T. Okamoto, *Energy Fuels* **10** (1996) 958–963.
7. M. Ishida, H. Jin, T. Okamoto, *Energy Fuels* **12** (1998) 223–229.
8. H. Jin, T. Okamoto, M. Ishida, *Energy Fuels* **12** (1998) 1272–1277.
9. H. Jin, T. Okamoto, M. Ishida, *Ind. Eng. Chem. Res.* **38** (1999) 126–132.
10. H. Jin, M. Ishida, *Ind. Eng. Chem. Res.* **41** (2002) 4004–4007.
11. T. Mattisson, A. Lyngfelt, P. Cho, *Fuel* **80** (2001) 1953–1962.
12. P. Cho, T. Mattisson, A. Lyngfelt, Reactivity of iron oxide with methane in a laboratory fluidised bed-application of chemical-looping combustion, *Seventh International Conference on Circulating Fluidised Beds*. Niagara Falls, Ontario, 2002, pp. 599–606.
13. T. Mattisson, A. Lyngfelt, P. Cho, Possibility of using iron oxide as an oxygen carrier for combustion of methane with removal of CO2, *Fifth International Conference on Greenhouse Gas Control Technologies*, 80, CSIRO, Cairns, 2001, 205–210.
14. T. Mattisson, A. Jardnas, A. Lyngfelt, *Energy Fuels* **17** (2003) 643–651.
15. A. Lyngfelt, B. Leckner, T. Mattisson, *Chem. Eng. Sci.* **56** (2001) 3101–3113.
16. R. Copeland, G. Alptekin, M. Cesario, Y. Gershanovich, Sorbent Energy Transfer System (SETS) for CO_2 separation with high efficiency, *The 27th International Technical Conference on Coal Utilization&Fuel Systems*, Clearwater, Florida, USA, 2002.
17. J. Adánez, L.F. de Diego, F. García-Labiano, P. Gayán, A. Abad, *Energy Fuels* **18** (2004) 371–377.
18. H.-J. Ryu, D.-H. Bae, K.-H. Han, S.-Y. Lee, G.-T. Jin, J.-H. Choi, *Korean J. Chem. Engng* **18** (2001) 831–837.
19. H.-J. Ryu, D.-H. Bae, G.-T. Jin, *Sixth International Conference on Greenhouse Gas Control Technologies*, Kyoto, Japan, 2002.
20. H.-J. Ryu, N.-Y. Lim, D.-H. Bae, G.-T. Jin, *Korean J. Chem. Engng* **20** (2003) 157–162.
21. K.S. Song, Y.S. Seo, H.K. Yoon, S.J. Cho, *Korean J. Chem. Engng* **20** (2003) 471–475.
22. H.-J. Ryu, D.-H. Bae, G.-T. Jin, *Korean J. Chem. Engng* **20** (2003) 960–966.
23. R. Villa, C. Cristiani, G. Groppi, L. Lietti, P. Forzatti, U. Cornaro, S. Rossini, *J. Mol. Catalyst A Chem.* **204–105** (2003) 637–646.
24. Lyngfelt, A., Thunman, H. Chapter 31 of this book.
25. C. Georgakis, C.W. Chang, Szekely, *J. Chem. Eng. Sci.* **34** (1979) 1072–1075.
26. J. Adánez, F. García-Labiano, L.F. de Diego, A. Plata, J. Celaya, P. Gayán, A. Abad, Optimizing the fuel reactor for chemical looping combustion, *17th International Conference on Fluidised Bed Combustion*, Jacksonville, Florida, 2003, Paper 63.
27. D. Kunii, O. Levenspiel, *Ind. Eng. Chem. Res.* **29** (1990) 1226–1234.